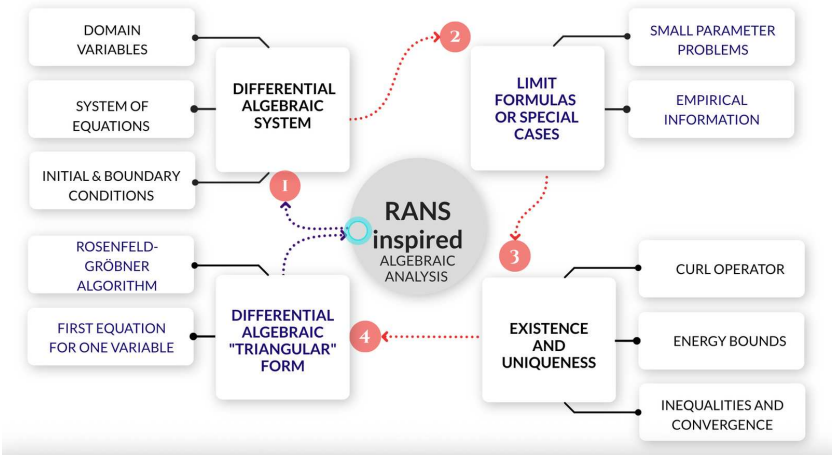


Graphical Abstract

Algebraic Reductibility Experiments of RANS-Inspired Equations

Carla Valencia, Sebastián Velasco, Manuel Romero de Terreros



Highlights

Algebraic Reductibility Experiments of RANS-Inspired Equations

Carla Valencia, Sebastián Velasco, Manuel Romero de Terreros

- Pressure-free rotational formulation
- *Rosenfeld–Gröbner* yields a triangular hierarchy
- Hierarchy accelerates training of physics-informed neural networks

Algebraic Reductibility Experiments of RANS-Inspired Equations

Carla Valencia^{a,*}, Sebastián Velasco^a, Manuel Romero de Terreros^{a,b}

^a*Universidad Iberoamericana Ciudad de México, Mexico City, 01219, Mexico*

^b*Vera Strata Research, Mexico City, 05100, Mexico*

Abstract

Prior to any statistical averaging we derive a rotational form of the Reynolds-Averaged Navier–Stokes (RANS) equations, which eliminates the pressure and exposes a velocity–vorticity interplay governed by

$$\partial_t(\boldsymbol{\omega} + \tilde{\boldsymbol{\omega}}) + (\boldsymbol{v} \cdot \nabla) \boldsymbol{\omega} + (\tilde{\boldsymbol{v}} \cdot \nabla) \tilde{\boldsymbol{\omega}} + (\boldsymbol{v} \cdot \nabla) \tilde{\boldsymbol{\omega}} + (\tilde{\boldsymbol{v}} \cdot \nabla) \boldsymbol{\omega} - \nu \Delta(\boldsymbol{\omega} + \tilde{\boldsymbol{\omega}}) = \mathbf{0}.$$

All terms are differential polynomials, so the system generates a differential–algebraic ideal. Using the *Rosenfeld–Gröbner* algorithm we obtain an equivalent triangular hierarchy whose first equation involves a single variable, the second at most two, and so on. This decoupling clarifies how prescribed mean-flow data drive the turbulent fluctuations and provides a hierarchy-ready foundation for physics-informed or physics-embedded neural networks. Energy estimates in Sobolev spaces complement the algebraic reduction and establish local well-posedness when the initial kinetic energy of the velocity and its curl is finite. The joint algebraic–energetic framework thus offers a pressure-free, computationally economical platform for data-driven turbulence analysis.

Keywords: Turbulence modelling, Navier–Stokes equations, Differential algebra, Rosenfeld–Gröbner, Physics-informed neural networks

2020 MSC: 35Q30, 76F55, 12H05, 35A01, 68T07

*Corresponding author

Email address: `carla.valencia@ibero.mx` (Carla Valencia)

1. Introduction

The study of turbulent flow, is pivotal in engineering applications, and the RANS equations remain central in its study [1, 2]. Turbulent motions in natural and built environments are rarely homogeneous: surface roughness patches, temperature gradients, and obstacles introduce spatial inhomogeneities that deflect a mean flow and seed multi-scale vortical structures. Capturing their dynamics is crucial for applications that range from atmospheric boundary-layer modelling to fluid–structure-interaction (FSI) assessments in extreme-event engineering.

Throughout this work we assume that the fluctuation field $\tilde{\mathbf{v}}$ possesses a clear physical interpretation: It captures the velocity deviations generated by environmental inhomogeneities, such as surface roughness, mosaics, temperature gradients and obstacles. arrays, etc.). One, \mathbf{v} corresponds to the classical velocity, and the other, $\tilde{\mathbf{v}}$, to the deflection caused by the active grid, both with null boundary conditions. This viewpoint provides a family of models able to describe and explain recent active-grid wind-tunnel experiments, in which controlled boundary perturbations produce atmospheric-like turbulence at unprecedented Reynolds numbers [3, 4, 5, 6, 7].

1.1 A pressure-free rotational RANS type expression

Starting from the instantaneous Navier–Stokes system we perform a two-scale split $\mathbf{u} = \mathbf{v} + \tilde{\mathbf{v}}$ before any averaging and apply the curl operator. The pressure term disappears, yielding the vorticity balance:

$$\partial_t(\boldsymbol{\omega} + \tilde{\boldsymbol{\omega}}) + (\mathbf{v} \cdot \nabla)\boldsymbol{\omega} + (\tilde{\mathbf{v}} \cdot \nabla)\tilde{\boldsymbol{\omega}} + (\mathbf{v} \cdot \nabla)\tilde{\boldsymbol{\omega}} + (\tilde{\mathbf{v}} \cdot \nabla)\boldsymbol{\omega} - \nu \nabla^2(\boldsymbol{\omega} + \tilde{\boldsymbol{\omega}}) = \mathbf{0}, \quad (1)$$

where $\boldsymbol{\omega} = \nabla \times \mathbf{v}$ and $\tilde{\boldsymbol{\omega}} = \nabla \times \tilde{\mathbf{v}}$. Equation (1) features one less variable than its primitive-variable counterpart and displays, term-by-term, how the mean profile and its curl steer the fluctuating vorticity and vice-versa through distinct cross-convective actions.

1.2 Differential-algebraic hierarchy

All operators in (1) act polynomially on the dependent variables, so the system forms a differential-algebraic ideal. Implementing the Rosenfeld–Gröbner algorithm [8, 9, 10, 11] we generate an equivalent triangular system

$$\mathcal{T}_1(\psi_1) = 0, \quad \mathcal{T}_2(\psi_1, \psi_2) = 0, \quad \mathcal{T}_3(\psi_1, \psi_2, \psi_3) = 0, \quad \dots$$

such that each block \mathcal{T}_k depends on at most k unknowns $\{\psi_1, \dots, \psi_k\}$. This cascading structure is particularly attractive for physics-informed neural networks (PINNs) or physics-embedded neural networks (PENNs), which can train each block separately, propagate automatic-differentiation residuals efficiently, and enforce hierarchical consistency.

1.3 Outline and contributions

Pressure elimination. Curling the momentum equations yields (1), reducing the state dimension and sharpening the velocity-only perspective.

Transparent coupling. The cross-advective terms in (1) make explicit how the mean field's initial/boundary data drive the fluctuating vorticity and vice-versa.

Triangular reduction. A Rosenfeld–Gröbner procedure produces a hierarchical representation with progressively fewer coupled variables, streamlining future neural-network solvers.

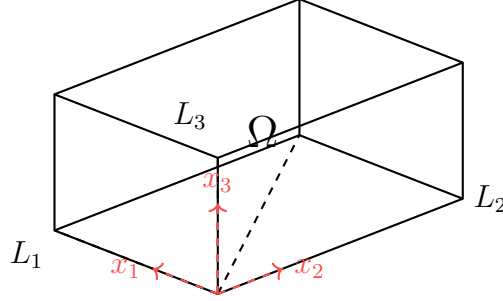
Because every term is a differential polynomial, the system defines a differential ideal. Section 5 applies the Rosenfeld–Gröbner algorithm [10, 11] to obtain equivalent triangular forms when for suitable cases. Section 3 derives Sobolev energy identities that combine with the algebraic reduction to give local existence and uniqueness in two and three dimensions. Conclusions and future directions close the paper.

2. Problem statement

Let $\Omega = (0, L_1) \times (0, L_2) \times (0, L_3) \subset \mathbb{R}^3$ with $L_i > 0$, $i = 1, 2, 3$. We split the velocity field as $\mathbf{u} = \mathbf{v} + \tilde{\mathbf{v}}$ with $\nabla \cdot \mathbf{v} = \nabla \cdot \tilde{\mathbf{v}} = 0$ and homogeneous Dirichlet data $\mathbf{v} = \tilde{\mathbf{v}} = \mathbf{0}$ on $\partial\Omega$. Define $\boldsymbol{\omega} := \nabla \times \mathbf{v}$ and $\tilde{\boldsymbol{\omega}} := \nabla \times \tilde{\mathbf{v}}$.

Remark 2.1. The following results are stated so that they may be extended to *starshaped* real domains Ω (where any ray with an origin in a fixed point has a unique common point with the topological boundary of the domain) and unknown solutions in a Sobolev space $W_p^k(\Omega)$, with $p \in \mathbb{N} - \{0\}$. This is possible thanks to the fact that the space of infinitely differentiable functions defined on the topological closure $\bar{\Omega} = \Omega \cup \partial\Omega$ of a starshaped domain Ω , denoted as $C^\infty(\bar{\Omega})$, is dense in $W_p^k(\Omega)$, where $\partial\Omega$ denotes the topological boundary of Ω . We denote $H^m(\Omega) := W_2^m(\Omega)$.

Remark 2.2. While a necessary and sufficient condition for a distribution in a Sobolev space to be the limit of a sequence of analytic functions is unknown it is possible to assume that the domain is starshaped with respect to a point to say that the space $C^\infty(\bar{\Omega})$ on a domain Ω is dense in the Sobolev space $W_p^k(\Omega)$ of distributions on Ω with derivatives of order $0 \leq l \leq k$ in the Lebesgue space $L_p(\Omega)$, for $p \in [1, \infty)$.



Remark 2.3. We may assume that the domain is a rectangular prism Ω and \mathbf{v} is an element of the space $C^\infty(\bar{\Omega})$ that satisfies both the Leibniz rule for the product derivative, the Gauss-Green formula [12, p. 699], and the generalisation of Schwarz's Theorem [12, p. 280] to exchange the order of the generalised second partial derivatives with respect to the spatial and temporal independent variables [13, 14], and perform an integration by parts process when needed. All differential identities below use that $\mathbf{v}, \tilde{\mathbf{v}} \in C^\infty(\bar{\Omega})$, vanish on $\partial\Omega$ and are divergence-free; hence surface integrals produced by integration-by-parts cancel, and Schwarz' theorem lets us swap mixed derivatives.

Theorem 2.4 (Rotational two-scale Navier-Stokes identity). *Fix a rectangular box*

$$\Omega = (0, L_1) \times (0, L_2) \times (0, L_3) \subset \mathbb{R}^3, \quad L_1, L_2, L_3 > 0,$$

and a finite time horizon $0 < T < \infty$. Let the pressure p and the velocity fields $\mathbf{v}, \tilde{\mathbf{v}} \in C^1([0, T]; C^\infty(\bar{\Omega}; \mathbb{R}^3))$ satisfy, for every $t \in [0, T)$,

- (i) **Boundary conditions :** $\mathbf{v} = \tilde{\mathbf{v}} = \mathbf{0}$ on $\partial\Omega$;
- (ii) **Incompressibility :** $\nabla \cdot \mathbf{v} = 0$ and $\nabla \cdot \tilde{\mathbf{v}} = 0$ in Ω ;
- (iii) **Momentum balance :**

$$\partial_t(\mathbf{v} + \tilde{\mathbf{v}}) + [(\mathbf{v} + \tilde{\mathbf{v}}) \cdot \nabla](\mathbf{v} + \tilde{\mathbf{v}}) = \nu \Delta(\mathbf{v} + \tilde{\mathbf{v}}) - \nabla p \quad \text{in } \Omega, \quad (2)$$

where $\nu > 0$ is the kinematic viscosity.

Define the mean and fluctuating vorticities

$$\boldsymbol{\omega} := \nabla \times \mathbf{v}, \quad \tilde{\boldsymbol{\omega}} := \nabla \times \tilde{\mathbf{v}}.$$

Then for all $(\mathbf{x}, t) \in \Omega \times (0, T)$ the pair $(\boldsymbol{\omega}, \tilde{\boldsymbol{\omega}})$ satisfies the rotational two-scale equation

$$\partial_t(\boldsymbol{\omega} + \tilde{\boldsymbol{\omega}}) + \underbrace{(\mathbf{v} \cdot \nabla)\boldsymbol{\omega} + (\tilde{\mathbf{v}} \cdot \nabla)\tilde{\boldsymbol{\omega}} + (\mathbf{v} \cdot \nabla)\tilde{\boldsymbol{\omega}} + (\tilde{\mathbf{v}} \cdot \nabla)\boldsymbol{\omega}}_{\text{four distinct advection terms}} - \nu \Delta(\boldsymbol{\omega} + \tilde{\boldsymbol{\omega}}) = \mathbf{0}. \quad (3)$$

In particular, the pressure has been eliminated and the dynamics are expressed solely in terms of the velocity fields and their curls.

Proof. Apply $\nabla \times (\cdot)$ to the momentum balance in (2) and use $\nabla \times \nabla p = \mathbf{0}$:

$$\partial_t(\boldsymbol{\omega} + \tilde{\boldsymbol{\omega}}) + \nabla \times ((\mathbf{v} + \tilde{\mathbf{v}}) \cdot \nabla)(\mathbf{v} + \tilde{\mathbf{v}}) = \nu \Delta(\boldsymbol{\omega} + \tilde{\boldsymbol{\omega}}).$$

Convection term. For any smooth vector fields \mathbf{a}, \mathbf{b} with $\nabla \cdot \mathbf{a} = 0$, $\nabla \times ((\mathbf{a} \cdot \nabla)\mathbf{b}) = (\mathbf{a} \cdot \nabla)(\nabla \times \mathbf{b})$. Splitting $\mathbf{v} + \tilde{\mathbf{v}}$ yields the four advection terms visible in (3).

Boundary-term elimination. Integrating each component over R and integrating by parts, all surface contributions vanish because $\mathbf{v} = \tilde{\mathbf{v}} = \mathbf{0}$ on ∂R . Hence the integral identity

$$\int_{\Omega} (\text{LHS of (3)}) \, d\mathbf{x} = \mathbf{0}$$

holds. By the mean-value theorem for integrals there exists $\mathbf{x}_0 \in \Omega$ where the integrand itself vanishes; smoothness then forces equality to hold pointwise, yielding (3). \square

Remark 2.5. Equation (3) is obtained under the *homogeneous (no-slip)* boundary conditions

$$\mathbf{v}|_{\partial\Omega} = \tilde{\mathbf{v}}|_{\partial\Omega} = \mathbf{0}.$$

Because both velocity fields vanish on $\partial\Omega$, every surface integral generated during the integration-by-parts steps cancels, the pressure term is eliminated, and only the four cross-advection couplings

$$(\mathbf{v} \cdot \nabla)\boldsymbol{\omega}, \quad (\tilde{\mathbf{v}} \cdot \nabla)\tilde{\boldsymbol{\omega}}, \quad (\mathbf{v} \cdot \nabla)\tilde{\boldsymbol{\omega}}, \quad (\tilde{\mathbf{v}} \cdot \nabla)\boldsymbol{\omega}$$

remain, making the transfer of initial or boundary data between $\boldsymbol{\omega}$ and $\tilde{\boldsymbol{\omega}}$ fully explicit. If either velocity field were non-zero on $\partial\Omega$, the boundary integrals would survive and additional terms, proportional to the prescribed boundary data, would have to be added to (3) for the identity to hold.

3. Energy bounds

Once the curl formulation (3) is in hand, we estimate the turbulent vorticity $\tilde{\omega} := \nabla \times \tilde{\mathbf{v}}$ in Sobolev norms. Throughout the section we assume that

$$\mathbf{v}, \tilde{\mathbf{v}} \in C^1([0, T]; C^\infty(\bar{\Omega}; \mathbb{R}^3)), \mathbf{v} = \tilde{\mathbf{v}} = \mathbf{0} \text{ on } \partial\Omega, \text{ and } \nabla \cdot \mathbf{v} = \nabla \cdot \tilde{\mathbf{v}} = 0.$$

3.1. Functional setting

For $\mathbf{f} = (f_1, f_2, f_3)$, $\mathbf{g} = (g_1, g_2, g_3) \in L^2(\Omega; \mathbb{R}^3)$ we use the standard inner product and norm

$$(\mathbf{f}, \mathbf{g})_0 := \int_{\Omega} \mathbf{f}(\mathbf{x}) \cdot \mathbf{g}(\mathbf{x}) \, d\mathbf{x}, \quad \|\mathbf{f}\|_0^2 := (\mathbf{f}, \mathbf{f})_0. \quad (4)$$

For a multi-index $\alpha = (\alpha_1, \alpha_2, \alpha_3) \in \mathbb{N}^3$ with $|\alpha| := \alpha_1 + \alpha_2 + \alpha_3 = k$, define the differential operator

$$D_{\alpha}^k := \frac{\partial^k}{\partial x_1^{\alpha_1} \partial x_2^{\alpha_2} \partial x_3^{\alpha_3}}, \quad D_{\alpha}^k \mathbf{f} := (D_{\alpha}^k f_j)_{j=1}^3.$$

3.2. Basic L^2 identities

If $\mathbf{f}, \mathbf{g} \in C^\infty(\bar{\Omega}; \mathbb{R}^3)$ satisfy $\mathbf{f}|_{\partial\Omega} = \mathbf{g}|_{\partial\Omega} = \mathbf{0}$ and $\nabla \cdot \mathbf{f} = 0$, then

$$(\partial_t \mathbf{f}, \mathbf{f})_0 = \frac{1}{2} \partial_t \|\mathbf{f}\|_0^2, \quad (5a)$$

$$((\mathbf{f} \cdot \nabla) \mathbf{f}, \mathbf{f})_0 = 0, \quad (5b)$$

$$((\mathbf{f} \cdot \nabla) \mathbf{g}, \mathbf{f})_0 = -((\mathbf{f} \cdot \nabla) \mathbf{f}, \mathbf{g})_0, \quad (5c)$$

$$(D_{\alpha}^k \Delta \mathbf{f}, D_{\alpha}^k \mathbf{g})_0 = -(\nabla D_{\alpha}^k \mathbf{f}, \nabla D_{\alpha}^k \mathbf{g})_0. \quad (5d)$$

Identities (5b)–(5c) follow from integration by parts and incompressibility; (5d) is Green's formula.

3.3. Energy balance for the fluctuation

Corollary 3.1 (Sobolev energy identity). *For every $k \in \mathbb{N}$ and $\alpha \in \mathbb{N}^3$ with $|\alpha| = k$,*

$$\begin{aligned} & \frac{1}{2} \partial_t \|D_{\alpha}^k \tilde{\omega}\|_0^2 + (D_{\alpha}^k \partial_t \omega, D_{\alpha}^k \tilde{\omega})_0 + (D_{\alpha}^k ((\mathbf{v} \cdot \nabla) \omega), D_{\alpha}^k \tilde{\omega})_0 \\ & + (D_{\alpha}^k ((\tilde{\mathbf{v}} \cdot \nabla) \tilde{\omega}), D_{\alpha}^k \tilde{\omega})_0 + (D_{\alpha}^k ((\mathbf{v} \cdot \nabla) \tilde{\omega}), D_{\alpha}^k \tilde{\omega})_0 \\ & + (D_{\alpha}^k ((\tilde{\mathbf{v}} \cdot \nabla) \omega), D_{\alpha}^k \tilde{\omega})_0 \\ & + \nu (\nabla D_{\alpha}^k \omega, \nabla D_{\alpha}^k \tilde{\omega})_0 + \nu \|\nabla D_{\alpha}^k \tilde{\omega}\|_0^2 = 0. \end{aligned} \quad (6)$$

In particular, for $k = 0$,

$$\frac{1}{2} \partial_t \|\tilde{\omega}\|_0^2 + (\partial_t \omega, \tilde{\omega})_0 + \nu (\nabla \omega, \nabla \tilde{\omega})_0 + \nu \|\nabla \tilde{\omega}\|_0^2 = 0, \quad (7)$$

because the four convective terms vanish by (5b)–(5c).

For planar, axisymmetric fields depending only on the radial coordinate ($\mathbf{v} = (v_1, v_2, 0)$, $\tilde{\mathbf{v}} = (\tilde{v}_1, \tilde{v}_2, 0)$), ω and $\tilde{\omega}$ reduce to a single (out-of-plane) scalar, and (7) simplifies further to

$$\frac{1}{2} \partial_t \|\tilde{\omega}\|_0^2 + (\partial_t \omega, \tilde{\omega})_0 = 0. \quad (8)$$

Proof. Apply D_α^k to the curl system (3), take the L^2 -inner product with $D_\alpha^k \tilde{\omega}$, and use identities (5). The Laplacian term is handled with (5d), yielding $\nu (\nabla D_\alpha^k \cdot, \nabla D_\alpha^k \cdot)$. For $k = 0$, all skew-symmetric advection products cancel, leaving (7). In the planar axisymmetric case $\nabla \times \mathbf{v}$ has only one component, eliminating the gradient terms and giving (8). \square

4. Energy bounds imply well-posedness

Corollary 4.1. *Let $\Omega \subset \mathbb{R}^3$ be a bounded C^∞ domain, and suppose the initial data*

$$\mathbf{v}_0, \tilde{\mathbf{v}}_0 \in H_\sigma^3(\Omega) := \{\mathbf{u} \in H^3(\Omega; \mathbb{R}^3) : \nabla \cdot \mathbf{u} = 0, \mathbf{u}|_{\partial\Omega} = \mathbf{0}\}$$

satisfy the finite-energy condition

$$\sum_{k=0}^3 \left(\|D^k \mathbf{v}_0\|_0^2 + \|D^k \tilde{\mathbf{v}}_0\|_0^2 \right) = E_0 < \infty.$$

Then there exists a time $T^ = T^*(E_0, \nu, \Omega) > 0$ and a unique pair of velocity fields*

$$(\mathbf{v}, \tilde{\mathbf{v}}) \in C([0, T^*]; H_\sigma^3(\Omega)) \cap L^2(0, T^*; H_\sigma^4(\Omega))$$

that solve the two-scale Navier–Stokes system (2) and its rotational form (3). Moreover,

$$\sup_{0 \leq t \leq T^*} \sum_{k=0}^3 \left(\|D^k \omega(t)\|_0^2 + \|D^k \tilde{\omega}(t)\|_0^2 \right) \leq C(E_0, \nu, \Omega),$$

and the solution depends Lipschitz-continuously on the initial data in $H_\sigma^3(\Omega)$.

Sketch of the proof. The Sobolev energy identity (6) with $k = 0, 1, 2, 3$ yields a closed differential inequality

$$\partial_t \mathcal{E}(t) + \nu \mathcal{D}(t) \leq C \mathcal{E}(t), \quad \mathcal{E}(t) := \sum_{k=0}^3 \left(\|D^k \boldsymbol{\omega}\|_0^2 + \|D^k \tilde{\boldsymbol{\omega}}\|_0^2 \right),$$

where the dissipation term $\mathcal{D}(t)$ is the sum of the corresponding H^{k+1} -seminorms. Bounding the all the cross-advection products by the Ladyzhenskaya and Gagliardo–Nirenberg inequalities [15, 16, 17] gives the constant $C = C(E_0, \nu, \Omega)$ and allows application of Gronwall’s lemma: $\mathcal{E}(t) \leq \mathcal{E}(0) e^{Ct}$. The *a priori* bound is therefore uniform up to a time T^* depending only on the initial energy and ν . Uniqueness follows by writing the equation for the difference of two solutions and repeating the same H^0 -energy estimate; the exponential bound and Gronwall imply the difference vanishes. \square

The next section shows how differential-algebra elimination triangularises the curl-system, paving the way for efficient PINN/PENN training.

5. Algebraic-reduction experiments

5.1. Motivation and theoretical background

During the last two decades algebraic techniques such as Gröbner bases [18, 19], *differential* Gröbner bases have opened a new route for analysing non-linear differential systems: one first rewrites the PDEs as a finite family of *differential polynomials* and then studies the associated *differential ideal*. A cornerstone of the theory is **Ritt’s finiteness theorem** which guarantees that every differential ideal admits a finite characteristic set in a suitable ranking [20, 21].

Consequently, many systems possess an *equivalent triangular form* whose first equation depends on a single dependent variable, the second equation on at most two variables, and so on. Besides revealing hidden algebraic structure, such triangularisations can dramatically reduce computational cost; see, e.g., the reductions obtained for the modified Chua circuit and the Rössler system in [22, p. 719]. Nowadays the most complete implementation of these ideas is the Rosenfeld–Gröbner algorithm of Boulrier and Lemaire [10, 11, 9]. Given a ranking, the algorithm returns a finite set of differential polynomials whose vanishing is equivalent to that of the original system; it is available in **Maple** and, recently, in a **Python** package.

5.2. Performance of the Rosenfeld–Gröbner algorithm on fluid models

The next table summarises our systematic runs of the algorithm on the main PDE families used in fluid mechanics. All computations were carried out in **Maple 2024** with the default elimination ranking, and convergence was declared when no new leaders appeared after 400 differential pseudo-reduction steps.

Model	C	In	S	E	St
Busemann jet	I	—	—	—	—
Prandtl boundary layer	—	R	—	—	—
Navier–Stokes (3-D)	I	I	R	I	I
RANS (3-D)	I	I	R	I	I
ω -RANS ^a	I	I	R	I	I
Stream-function NS (2-D)	—	R	—	—	R

Table 1: Algebraic reducibility obtained with the Rosenfeld–Gröbner algorithm (default ranking). Codes: **R** – reducible (finite triangular characteristic set), **I** – irreducible (algorithm keeps generating higher-order derivatives), — – model/class not applicable. Column headings: **C** = compressible, **In** = incompressible, **S** = Stokes limit, **E** = Euler limit, **St** = stationary (time-independent).

Two main observations emerge:

- With the exception of the two-dimensional stream-function formulation, neither the Navier–Stokes nor the classical RANS equations admit a finite triangularisation in three dimensions. Empirically, the convective derivative $(\mathbf{v} \cdot \nabla)\mathbf{v}$ propagates ever higher mixed derivatives and prevents convergence.
- When the convective term is *absent* (Stokes limit) or when the vorticity is described by a single scalar potential (stream-function ψ in 2-D), the algorithm terminates and produces an explicit triangular form.

5.3. Illustrative triangularisations

The symbol $>$ denotes the ranking order chosen for the variables.

Example 1. *Incompressible Stokes in 3-D.* Consider the Stokes system. This is, $(\mathbf{v} \cdot \nabla)\mathbf{v} = 0$, $\mathbf{v} = (u, v, w)$, p is the pressure, and:

$$\Sigma_1 : \begin{cases} u_x + v_y + w_z = 0, \\ u_t + p_x - \nu \Delta u = 0, \\ v_t + p_y - \nu \Delta v = 0, \\ w_t + p_z - \nu \Delta w = 0. \end{cases} \quad (\Sigma_1)$$

With ranking $u > v > w > p$ the algorithm produces the triangular set

$$\begin{aligned} u_x &= -v_y - w_z, \\ p_{xx} &= -p_{yy} - p_{zz}, \\ w_{xx} &= -w_{yy} - w_{zz} + \nu^{-1}(p_z + w_t), \\ v_{xx} &= -v_{yy} - v_{zz} + \nu^{-1}(p_y + v_t), \\ u_{yy} &= -u_{zz} + v_{xy} + w_{xz} + \nu^{-1}(p_x + u_t). \end{aligned}$$

Each equation involves at most one new leader, so the system is now *triangular* and can be solved sequentially.

Example 2. *Incompressible RANS with fluctuating field..* Let \mathbf{v} be the mean velocity and $\mathbf{v}' = (u', v', w')$ the fluctuations. Under the Stokes hypothesis the RANS system is

$$\Sigma_2 : \begin{cases} u_x + v_y + w_z = 0, \\ u_t + u'_t + p_x - \nu \Delta(u + u') = 0, \\ v_t + v'_t + p_y - \nu \Delta(v + v') = 0, \\ w_t + w'_t + p_z - \nu \Delta(w + w') = 0. \end{cases} \quad (\Sigma_2)$$

Using the ranking $u > v > w > u' > v' > w' > p$ the resulting characteristic set begins with

$$\begin{aligned} u_x &= -v_y - w_z, \\ u'_{xxx} &= -u'_{xyy} - u'_{xzz} - v'_{xxy} - v'_{yyy} - v'_{yzz} - w'_{xxz} - w'_{yyz} - w'_{zzz} \\ &\quad + \nu^{-1}(p_{xx} + p_{yy} + p_{zz} + u'_{tx} + v'_{ty} + w'_{tz}), \\ w_{xx} &= -\Delta w - \Delta w' + \nu^{-1}(p_z + w'_t + w_t), \end{aligned}$$

and analogous relations for v_{xx} and u_{yy} . Although not fully decoupled, the triangular structure shows that all spatial derivatives can ultimately be written

in terms of p and time derivatives, providing a much sparser representation than the original PDE set.

These examples confirm the practical relevance of differential–algebra tools: whenever the convective non-linearity is absent or bypassed (e.g. by introducing a stream function in 2-D) a finite triangular characteristic set emerges and can be leveraged for further qualitative or numerical analysis. Extending these reductions to the full 3-D Navier–Stokes and ω -RANS systems remains an open challenge.

5.4. Examples of Differential Polynomial Systems

We consider a system Σ_n of polynomial differential equations, where Σ_1 represents the set of differential equations of three-dimensional Navier Stokes for incompressible fluids under Stokes' condition $(\mathbf{v} \cdot \nabla)\mathbf{v} = 0$, where u, v, w are the velocity components, p is the pressure and ν is the kinematic viscosity:

$$\Sigma_1 = \begin{cases} u_x + v_y + w_z = 0, \\ u_t + p_x - \nu(u_{xx} + u_{yy} + u_{zz}) = 0, \\ v_t + p_y - \nu(v_{xx} + v_{yy} + v_{zz}) = 0, \\ w_t + p_z - \nu(w_{xx} + w_{yy} + w_{zz}) = 0. \end{cases} \quad (9)$$

For Σ_1 with a *ranking* $u > v > w > p$, we obtain a reduction:

$$u_x = -v_y - w_z, \quad (10)$$

$$p_{x,x} = -p_{y,y} - p_{z,z}, \quad (11)$$

$$w_{x,x} = -w_{y,y} - w_{z,z} + \nu^{-1}p_z + \nu^{-1}w_t, \quad (12)$$

$$v_{x,x} = -v_{y,y} - v_{z,z} + \nu^{-1}p_y + \nu^{-1}v_t, \quad (13)$$

$$u_{y,y} = -u_{z,z} + v_{x,y} + w_{x,z} + \nu^{-1}p_x + \nu^{-1}u_t. \quad (14)$$

Σ_2 represents the set of differential of three dimensional RANS equations for incompressible fluids under Stokes' condition $(\mathbf{v} \cdot \nabla)\mathbf{v} = 0$, where u, v, w are the averaged velocity components, u', v', w' are the fluctuations of the velocities, p is the pressure and ν is the kinematic viscosity:

$$\Sigma_2 = \begin{cases} u_x + v_y + w_z = 0, \\ p_x + u_t + u'_t - \nu(u_{xx} + u_{yy} + u_{zz} + u'_{xx} + u'_{yy} + u'_{zz}) = 0, \\ p_y + v_t + v'_t - \nu(v_{xx} + v_{yy} + v_{zz} + v'_{xx} + v'_{yy} + v'_{zz}) = 0, \\ p_z + w_t + w'_t - \nu(w_{xx} + w_{yy} + w_{zz} + w'_{xx} + w'_{yy} + w'_{zz}) = 0. \end{cases} \quad (15)$$

Furthermore, for Σ_2 with a *ranking* $u > v > w > u' > v' > w' > p$, we obtain a reduction:

$$u_x = -v_y - w_z; \quad (16)$$

$$\begin{aligned} u'_{x,x,x} = & -u'_{x,y,y} - u'_{x,z,z} - v'_{x,x,y} - v'_{y,y,y} - v'_{y,z,z} - w'_{x,x,z} - w'_{y,y,z} - w'_{z,z,z} \\ & + \nu^{-1}(p_{x,x} + p_{y,y} + p_{z,z} + u'_{t,x} + v'_{t,y} + w'_{t,z}); \end{aligned} \quad (17)$$

$$w_{x,x} = -w'_{x,x} - w'_{y,y} - w'_{z,z} - w_{y,y} - w_{z,z} + \nu^{-1}(p_z + w_{1t} + w_t); \quad (18)$$

$$v_{x,x} = -v'_{x,x} - v'_{y,y} - v'_{z,z} - v_{y,y} - v_{z,z} + \nu^{-1}(p_y + v'_t + v_t); \quad (19)$$

$$u_{y,y} = -u'_{x,x} - u'_{y,y} - u'_{z,z} - u_{z,z} + v_{x,y} + w_{x,z} + \nu^{-1}(p_x + u'_t + u_t). \quad (20)$$

6. Conclusions

The algebraic viewpoint adopted in this work complements — rather than competes with — classical energy techniques. Its main contributions and implications are summarised in Table 2; subsequent paragraphs outline near-term research avenues.

Directions opened by the present study

Functional duals of differential ideals. We are constructing functionals whose vanishing differential coincides with the ideal annihilating the convective term, aiming at a systematic functional–ideal dictionary.

Algebraic phase diagram of fluid models. A classification (reducible vs. irreducible) as a function of dimension, forcing and transport structure would streamline reduced-order model selection.

Three-dimensional regularity via maximum principles. Oleĭnik-style parabolic principles, together with the ω – $\tilde{\omega}$ symmetry, are being investigated as an alternative to Galerkin in $d = 3$.

Symbolic detection of periodic orbits. The rational-solution counter for differential polynomial systems will be used to identify low-period attractors in the reduced two-dimensional equations, providing stringent benchmarks for data-driven closures.

Key finding**Impact / interpretation**

Triangular reductions (via Rosenfeld–Gröbner) are achievable for Prandtl, Stokes and other models *when the convective term is absent*.

An upper-triangular form permits single-variable marching, lowering algebraic stiffness and paving the way for efficient PINN training.

Irreducibility correlates with the *presence* of $(\mathbf{v} \cdot \nabla)\mathbf{v}$, not with turbulence, compressibility or dimension alone.

Points to where modelling or pre-processing effort should focus if algebraic reduction is desired.

Each “stubborn” convective product is the very term controlled by Gagliardo–Nirenberg / Ladyzhenskaya in the energy proof.

Hints at a duality: *algebraic reducibility \iff existence of a coercive energy functional*.

In vorticity form, fluctuations $\tilde{\omega}$ are driven solely by the classical curl ω ; pressure is eliminated.

Enables direct bounding or forecasting of $\tilde{\omega}$ once ω is known from LES/DNS or coarse PINNs.

Even partial (non-triangular) eliminations expose repeated differential patterns useful as physics-aware features.

Early experiments show faster PINN convergence and better generalisation when these features are injected.

Table 2: Principal outcomes of the algebraic–energetic analysis.

Algebraic elimination is not an after-thought for fluid dynamics; when paired with energy methods it becomes a rigorous roadmap towards both deeper analysis and more economical computation of turbulent flows.

Acknowledgements

The authors gratefully acknowledge the financial support received from: Universidad Iberoamericana, Ciudad de México, for the 18th Scientific Research Call. We are very grateful for their backing on this project.

References

- [1] Y. Tominaga, CFD simulations of turbulent flow and dispersion in built environment: a perspective review, *J. Wind Eng. Ind. Aerodyn.* 249 (2024) 105741.
- [2] C. Meneveau, Big wind power: seven questions for turbulence research, *J. Turbul.* 20 (2019) 1–19.
- [3] L. Neuhaus, M. Hölling, W.J.T. Bos, J. Peinke, Generation of atmospheric turbulence with unprecedentedly large Reynolds number in a wind tunnel, *Phys. Rev. Lett.* 125 (2020) 154503.
- [4] L. Neuhaus, F. Berger, J. Peinke, et al., Exploring the capabilities of active grids, *Exp. Fluids* 62 (2021) 130.
- [5] O. Kildal, L. Li, R.J. Hearst, Ø.W. Petersen, O. Øiseth, On the use of an active turbulence grid in wind tunnel testing of bridge decks, *J. Wind Eng. Ind. Aerodyn.* 233 (2023) 105331.
- [6] J. Kistner, L. Neuhaus, N. Wildmann, High-resolution wind speed measurements with quadcopter uncrewed aerial systems: calibration and verification in a wind tunnel with an active grid, *Atmos. Meas. Tech.* 17 (2024) 4941–4955.
- [7] S. Angriman, S.E. Smith, P. Clark di Leoni, P.J. Cobelli, P.D. Mininni, M. Obligado, Active grid turbulence anomalies through the lens of physics-informed neural networks, *Results Eng.* 24 (2024) 103265.
- [8] F. Boulier, Étude et implantation de quelques algorithmes en algèbre différentielle, Ph.D. Thesis, Université de Lille I, 1994.
- [9] F. Boulier, D. Lazard, F. Ollivier, M. Petitot, Representation for the radical of a finitely generated differential ideal, in: *Proc. ISSAC*, ACM, 1995, pp. 158–166.
- [10] F. Boulier, F. Lemaire, Computing canonical representatives of regular differential ideals, in: *Proc. ISSAC*, ACM Press, 2000, pp. 38–47.
- [11] F. Boulier, D. Lazard, F. Ollivier, M. Petitot, Computing representations for radicals of finitely generated differential ideals, *Appl. Algebra Eng. Commun. Comput.* 20 (2009) 73–121.

- [12] N. Piskunov, *Differential and Integral Calculus*, Mir Publishers, Moscow, 1969.
- [13] V.G. Maz'ya, S.V. Poborchii, *Differentiable Functions on Bad Domains*, World Scientific, 1997.
- [14] V. Maz'ya, *Sobolev Spaces*, Springer, Berlin, 2013.
- [15] Bressan A., *Lecture Notes on Sobolev Spaces*, February 27, 2012.
- [16] Adams, R. A., *Sobolev Spaces*, Academic, New York, 1975.
- [17] Majda A., Bertozzi A. L., *Vorticity and Incompressible Flow*, Cambridge University Press, 2002.
- [18] B. Buchberger, What is a Gröbner basis?, *Not. Am. Math. Soc.* 52 (2005) 1199–1200.
- [19] B. Buchberger, An algorithm for finding the basis elements of the residue class ring of a zero dimensional polynomial ideal, *J. Symb. Comput.* 41 (2006) 475–511.
- [20] J.F. Ritt, *Differential Algebra*, Dover Publications, New York, 1950.
- [21] E.R. Kolchin, *Differential Algebra and Algebraic Groups*, Academic Press, New York, 1973.
- [22] H.A. Harrington, R.A. van Gorder, Reduction of dimension for nonlinear dynamical systems, *Nonlinear Dyn.* 88 (2017) 715–734.